AAN031

# Evaluation of nonlinear LAOS experiments

Aly Franck, TA Instruments, Germany

Keywords: LAOS, Fourier Rheology, DFT, Fourier coefficients, elastic & viscous stress, Nonlinear viscoelasticity, strain sweep


## ABSTRACT

The nonlinear stress response upon a sinusoidal strain input on the ARES-G2 can be recorded and analyzed in two ways: 1. Fast sampling of the stress as a function of time followed by discrete Fourier analysis (DFT) or decomposition of the stress signal into an elastic and viscous component. 2. Direct correlation of the measured stress and the input strain to determine the magnitude and phase of the fundamental and harmonics up to the 9th order. This method can be conveniently integrated into standard test modes such as time, strain or frequency sweeps which provide the desired results (dynamic moduli $G'_n$. $G''_n$ or magnitude ratio $I_n(\omega_n)/I_1(\omega))$ immediately.

Nonlinear oscillation measurements of a 4wt% Xanthan gum solution have been performed as a function of strain amplitude. Fourier coefficients of the stress signal are evaluated by direct correlation, discrete Fourier transformation and decomposition of the measured stress in a contribution in phase with the strain and one in phase with the strain rate. The results are compared and analyzed in terms of reproducibility and accuracy of the method. Structural changes during the transition from linear to nonlinear behavior are discussed based on elastic and viscous deformation mechanisms.


## INTRODUCTION

During an oscillation experiment on a Separate Motor Transducer (SMT) rheometer, a sinusoidal deformation is applied to the material. As long as the total deformation is small, linear viscoelasticity prevails and the measured stress at steady state remains sinusoidal. In order to evaluate the material's response, the stress is decomposed into two wave functions, one in phase with the strain and one in phase with the strain rate. In analogy to a solid material (strain and stress are in phase) and a simple fluid (strain rate and stress are in phase), the part in phase with the strain represents the elastic (solid like) deformation behavior, the part in phase with the strain rate (out of phase with the strain) is the viscous (fluid like) behavior. As such, the stress can be expressed by the sum of the two components as follows:

$$\sigma(t) = \sigma'(t) + \sigma''(t) \quad (1)$$

Instead of representing the stress and strain versus time explicitly, the stress can be plotted against the strain directly (Figure 1). As long as the measured stress wave is sinusoidal the stress describes an ellipsoid in this representation, also referred to as "Lissajous" representation[1]. When the stress is in-phase with the strain, the ellipsoid collapses to a straight line through the origin.

When the stress response of the material upon a sinusoidal strain input is not a simple sinusoidal function, the material behaves nonlinear and the ellipsoid in the stress-strain representation changes to a more complex geometrical shape. The nonlinear stress response for example can

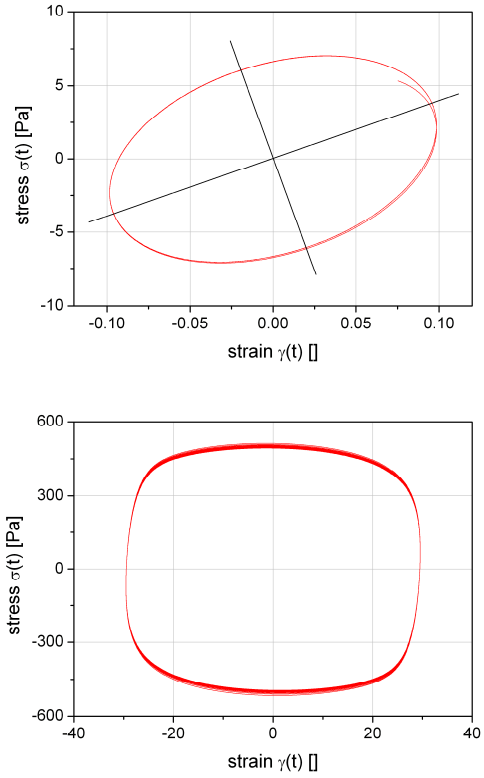


*Figure 1: Lissajous representation of the measured stress response upon a sinusoidal strain input in case of linear (upper) and nonlinear (lower) response for a PIB solution*

be developed in a Fourier series according to:

$$\sigma(t,\omega,\gamma_o) = \gamma_o \sum_{n=odd} \left\{ \begin{matrix} G_n'(\omega,\gamma_o)\sin n\omega t + \\ G_n''(\omega,\gamma_o)\cos n\omega t \end{matrix} \right\} \quad (2)$$

and in complex notation:

$$\sigma(t,\omega,\dot{\gamma}_o) \propto \sum_{n=odd}^{\infty} a_n e^{i(n\omega t+\phi_n)} \quad (3)$$

Although the Lissajous figure represents an excellent visual aid for qualitative analysis, it is difficult to use when a quantitative evaluation is required. In this case it is more convenient to extract the various components of the stress response by Fourier transformation. The Fourier transformation decomposes the stress signal and produces a frequency spectrum represented by the fundamental and higher order odd harmonics[2]. Each peak in the spectrum is characterized by a magnitude $a_n$ and a phase $\phi_n$. Although this mathematical analysis of nonlinear signals provides a complete description of the stress response; it is difficult a priori to associate the results from the Fourier analysis with physical material properties. The dynamic modulus $G'$, representing the elastic nature of a material and $G''$, representing the viscous dissipation of energy in the linear region lose their physical meaning. In analogy to the linear viscoelasticity, the components of the nonlinear response in phase with the strain and in

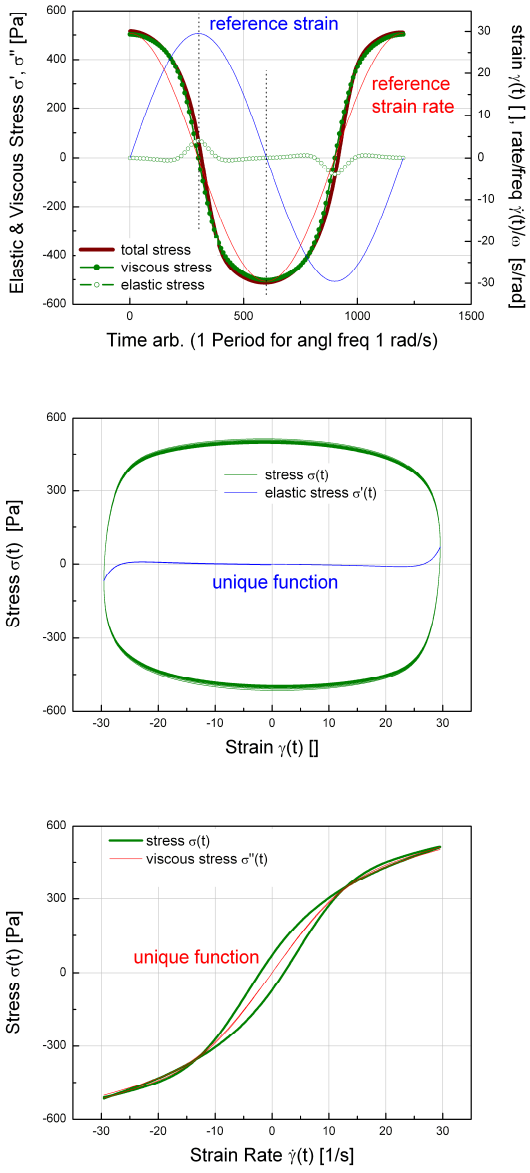


*Figure 2: Representation of the measured stress, the viscous and elastic stress for a PIB solution plotted versus time, strain and strain rate tested at 3000% strain and a frequency of 1 rad/s.*

phase with the strain rate can be interpreted as elastic and viscous stress[3]. Based on symmetry arguments, the measured stress can be decomposed into an elastic stress component $\sigma'$ and a viscous stress component $\sigma''$ (Figure 2). Both stress components $\sigma'$ and $\sigma''$ are unique functions (single curve in the Lissajous representation) of strain i.e. strain rate. The elastic and viscous stress components can be conveniently fitted by Chebyshev polynomials of the first kind[4]. The higher order Chebyshev coefficients ($e_n, v_n$) are excellent parameters to describe intra-cycle changes of the elastic and viscous stress. A positive $e_3$ (3rd order coefficient) corresponds to an increase of the maximum elastic stress (intra-cycle strain stiffening), a negative $e_3$ to a decrease of the maximum elastic stress (intra-cycle strain softening). The Chebyshev coefficients are related to the Fourier coefficients ($G'_n$, $G''_n$)[5] in a simple way according to:

$$e_n = G'_n(-1)^{(n-1)/2} \qquad (n=odd)$$
$$v_n = \frac{G''_n}{\omega} = \eta'_n \qquad (4)$$

In the linear regime, all higher order coefficients disappear and $e_1$ represents $G'$, the linear viscoelastic storage modulus and $v_1\omega$ represents $G''$, the loss modulus. The same physical interpretation of $e_3$ can be attached to $G'_3$, the 3rd order Fourier coefficient and so on – thus providing physical meaning to the higher harmonic coefficients obtained from correlation i.e. Fourier transform techniques, commonly used in commercial rheometers.

## EXPERIMENTAL

Oscillation rheometers generate test results in terms of elastic and viscous modulus from dynamic mechanical experiments by evaluating $G'_1$ and $G''_1$, the first order Fourier coefficients. Because of increasing interest in highly nonlinear material behavior, an easy to use approach to evaluate the results obtained under large oscillation strains (LAOS) is needed. A number of investigations have been conducted in this respect in the nonlinear viscoelastic region under large oscillation strain conditions[6, 7, 8] using discrete Fourier transformation to evaluate the stress response.

The special feature of the new ARES-G2 rheometer, based on the unique SMT technique is to perform experiments at large oscillation strains and to measure the material's response with the accuracy and temporal resolution necessary to allow a quantitative analysis of the higher order harmonic contributions of the raw stress signal. The rheometer uses a data acquisition system which incorporates fast acquisition channels for displacement, torque, normal force and an auxiliary signal with a sampling rate of 8kHz each. Pre-averaging based on oversampling techniques further improves the signal to noise ratio of the raw signals. The ARES-G2 provides two methods to analyze the oscillation data:

1. Real time correlation to determine magnitude and phase of the fundamental and the higher order components during the test. In this mode results up to the 9th order harmonic contribution can be obtained simultaneously. The advantage of this approach is the full integration into the existing methodology of performing oscillation tests. Higher harmonic analysis can be selectively checked in the correlation settings of all standard oscillation test modes.
2. Post-processing of the raw strain and stress data using discrete Fourier transformation (DFT) after previous sampling and saving the raw signals. A new test mode, the "SineTransient" collects the raw oscillation stress (shear and/or normal) and strain data as a function of time. The maximum order for the harmonic evaluation is not limited and can be selected based on the significance of the magnitude of the harmonics.

The material used in this investigation is a 4wt% aqueous solution of Xanthan gum (Sigma-Aldrich Co.). The sample was dissolved in purified water over night and vigorously stirred for several hours.

The rheological measurements were performed using a 50mm diameter stainless steel cone plate geometry with a cone angle of 0.04rad and a cone truncation of 50$\mu$m. Oscillation strain sweep experiments were conducted from $10^{-4}$ to 100 strain units. The correlation conditions for each data point were: 10 cycles delay and 10 cycles for correlation. The $n^{th}$ order harmonic is obtained by correlating the measured stress and strain signals with two out of phase reference signals at *n*-times the fundamental frequency. The test (strain excitation) frequency in this study is 1 Hz. The phase and the magnitude of the fundamentals and the odd harmonics ($3^{rd}$, $5^{th}$, $7^{th}$, and $9^{th}$) were recorded. In a second step, SineTransient experiments at fixed frequency and strain amplitude were performed in the range from 0.01 to 63 strain units. The correlation conditions were chosen to be the same as those for the strain sweep experiment: 10 cycles delay and 10 cycles for data sampling. The sampling rate for all measured signals was 1000 pts/s. The stress and strain signals are converted using a discrete Fourier transformation routine (DFT) to extract magnitude and phase for all significant harmonic contributions and the Fourier coefficients $G'_n$ and $G''_n$ were calculated according to equation 2. The same set of data was also evaluated using the MITLAOS package[9] to determine the Chebyshev coefficients. The same order of harmonic contributions was used in both evaluations.

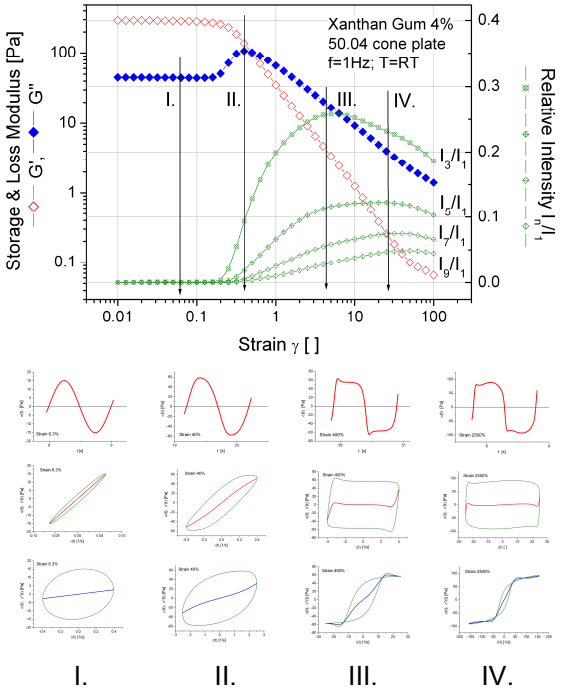


*Figure 3: Strain sweep of a Xanthan gum (4wt%) solution with the dynamic modulus G' and G" as well as the relative magnitudes of the 3rd, 5th, 7th and 9th harmonic stress contributions.*

## RESULTS

### Analysis of the results from the strain sweep experiment

Figure 3 shows the storage and loss modulus ($G'$, $G''$) of the Xanthan gum solution as a function of the strain amplitude $\gamma_0$. Beyond 20% strain $G'$ decreases; $G''$ initially increases slightly then decreases, however at a lower pace. The response with a weak $G''$ overshoot is a type III behavior according to the classification proposed by Hyun *et al.*[10]. The same graph includes the magnitudes of the higher harmonic stress contributions, reduced to relative intensities according to (Index 1 represents the fundamental):

$$\frac{I_n}{I_1} = \frac{|\sigma_n^*|}{|\sigma_1^*|} \qquad (5)$$

In the linear region (below 20% strain), the magnitudes of the higher harmonic contributions are zero. At the onset of the nonlinear response, the magnitude of the $3^{rd}$ harmonic stress increases sharply. The shape of the stress waveform in this region is tilted backwards and asymmetric in respect to a vertical line through the mid point. In the region characterized by a steady decrease of $G'$ and $G''$ at ~ 600% strain, the relative magnitude of the $3^{rd}$ harmonic stress decreases again. The shape of

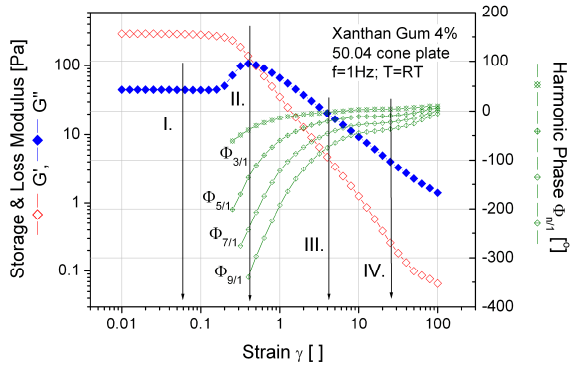


*Figure 4: Strain sweep of a Xanthan gum (4wt%) solution showing the dynamic modulus G' and G" as well as the harmonic phase of the 3rd, 5th, 7th and 9th harmonic stress contributions*

the stress waveform has changed significantly, shows a flat plateau and has partially recovered its symmetry. The relative magnitudes of the 5th, 7th and 9th harmonic stress follow the same trend, however they do appear at a higher strain and the magnitude is less pronounced.

Below figure 3 the Lissajous figures, representing the stress vs. strain and strain rate at 4 strain amplitudes from the linear into the nonlinear region are shown. In the linear region I, the stress vs. strain and strain rate represent ellipsoids. The elastic stress $\sigma'(\gamma(t))$, in phase with the strain and the viscous stress $\sigma''(\dot{\gamma}(t))$, in phase with the strain rate are unique functions and represent straight lines through the origin. With increasing strain the ellipsoids are tilted. The elastic and viscous stress remain unique functions, but they cannot be represented by a straight line anymore. Higher order Fourier coefficients are necessary to describe the viscous and elastic stress.

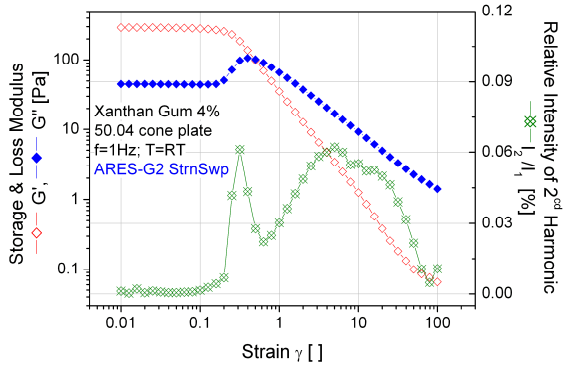


*Figure 5: Strain sweep of a Xanthan gum (4wt%) solution showing the dynamic modulus G' and G" as well as the relative magnitude of the 2nd harmonic stress contribution*

In figure 4 the phase of the higher harmonic stress contributions is plotted vs. strain amplitude. The harmonic phase is the phase, referred to the fundamental stress. The new time reference is established according to Neidhöfer *et al*. by substituting $t$ by $t' - \phi/\omega$ for the measured stress response[11]. The stress in eq. 2 can be reformulated as:

$$\sigma(t',\omega,\dot{\gamma}_o) \propto \sum_{n=odd} a_n \sin(n\omega t' + \Phi_n) \qquad (6)$$

with $\Phi_n = \phi_n - n\phi_1$

(n=1 refers to the fundamental frequency, ω is the excitation frequency). The phase of the dominating 3rd harmonic is significant for the symmetry of the experimental stress waveform. A harmonic phase $\Phi_3$ of 270° (-90°) tilts the waveform backwards with a shoulder to the left[11]. A harmonic phase $\Phi_3$ of 0° restores the symmetry of the waveform, but reduces the amplitude maximum and flattens the stress maximum to a broad plateau.

Even harmonic contributions of the stress response are not expected since the stress response is symmetric with respect to the shear strain or shear rate, which means that the material's response is the same in both shear directions. The magnitude of the 2nd harmonic in figure 5 however shows a small sharp peak at the onset of the nonlinear behavior and a broader peak at higher strain amplitude. The contribution of the 2nd harmonic stress is indeed small (0.06%) in comparison to those of the odd harmonics (20%). Even harmonics can result from secondary flows[13] or wall slip[14]. The latter is probably the reason for the appearance of the small 2nd harmonic contribution since no special precautions have been made to eliminate slip at the plate surface.

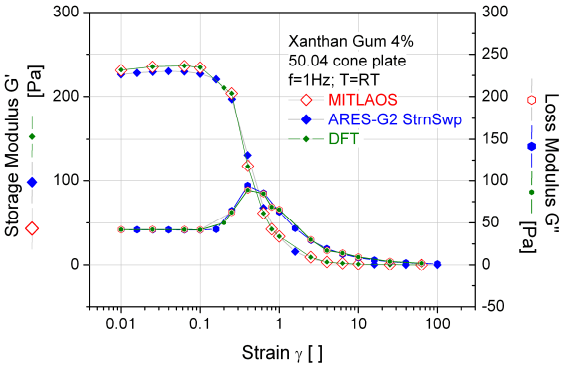


*Figure 6: Comparison of Storage and Loss modulus determined in the strain sweep experiment with the first order Fourier coefficients obtained from the DFT and MITLAOS programs of the raw stress and strain signals.*

## Analysis of the results from the Sine Transient experiments

Time dependent stress and strain data have been collected at discrete stain amplitudes of 1%, 3%, 6.3%, 10%, 30%, up to 6300%. The Fourier coefficients $G'_n$, $G''_n$ were calculated from the magnitude and the phase of the harmonic stress contributions obtained from discrete Fourier transformation of the stress and strain waves. In order to compare with the results of the strain sweep experiments, the Fourier coefficients were also calculated from the magnitude and phase determined by the rheometer according to:

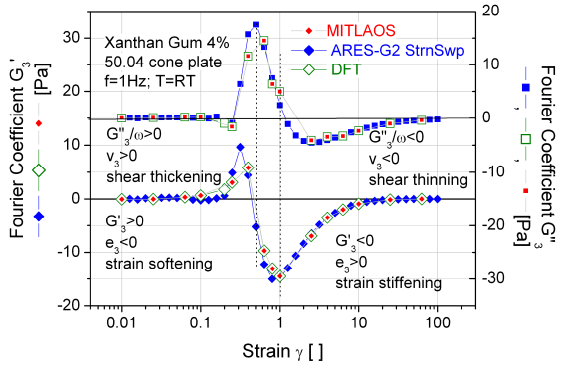


*Figure 7: 3rd harmonic Fourier Coefficients G'3, G"3 as a function of the strain amplitude*

$$G_n^{'} = \frac{|\sigma_n^*|}{\dot{\gamma}_o}\sin\delta_n$$

$$G_n^{''} = \frac{|\sigma_n^*|}{\dot{\gamma}_o}\cos\delta_n \qquad (7)$$

with $\delta_n = \phi_n - n\phi_s$

$\delta_n$ is the phase referred to the fundamental strain, $\phi_n$, $\phi_s$ the experimental phases of the harmonic stress contributions and the strain.

The Fourier coefficients were also calculated from the Chebyshev coefficients determined with the MITLAOS(*) program, developed by Ewoldt *et al.* [9] according to equation 4.

The first order Fourier coefficients represent the linear viscoelastic storage ($G_1$') and loss ($G_1$") modulus and are plotted in figure 6 as a function of the strain amplitude. The results calculated using the DFT and MITLAOS programs agree very well with the data from the strain sweep experiments. This is to be expected as the same Xanthan gum sample was tested under merely the same experimental conditions.

Figure 7 is the same plot for the 3rd Fourier coefficient. Similar to the results for the 1st Fourier coefficients, excellent agreement has been obtained for $G'_3$, $G''_3$ using the 3 evaluation methods (Correlation, DFT and MITLAOS). In the linear region, below 20% strain, the contributions of the 3rd harmonic are zero. At the onset of the nonlinear behavior, $G'_3$ increases to a maximum at 30% strain and then rapidly decreases to negative values to reach its minimum value at approximately 100% strain. This means that the elastic Chebyshev coefficient $e_3$, initially becomes negative and turns positive at higher strain amplitude (Note, the sign changes for the 3rd harmonic contribution in eq. 4.). A positive 3rd Chebyshev coefficient provides an increase of the

(*)MITLAOS uses FFT to calculate Chebyshev coefficients. This avoids the complex multistep decomposition of the stress and the numerical integrations to obtain $e_n$ and $v_n$

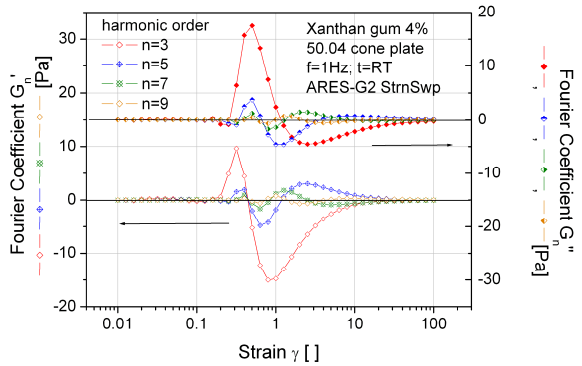


*Figure 8: The elastic and viscous Fourier coefficients for all odd harmonics of the order 3 to 9 are shown as a function of strain. The significance decreases with increasing order*

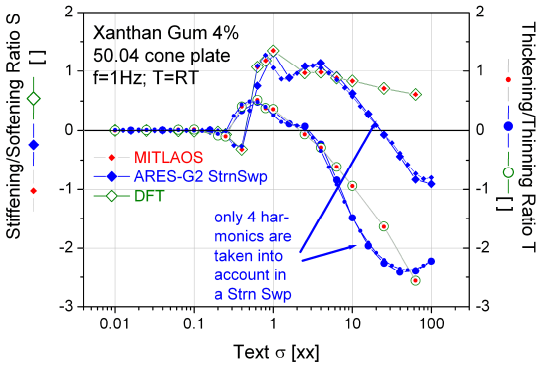


*Figure 9: Elastic strain-stiffening/softening and viscous shear-thickening/thinning ratio for the 4wt% Xanthan gum gel during the transition from linear to nonlinear behavior .*

maximum elastic stress, which stands for an "intra-cycle" strain stiffening effect [4].

The viscous Fourier coefficient $G''_3$ slightly drops to become negative at the onset of the nonlinear behavior and increases significantly to a high positive maximum value around 50% strain, followed by a sharp drop to a negative minimum at approximately 200% strain. The viscous Chebyshev coefficient $v_3$ is directly proportional to the viscous Fourier coefficient. A positive viscous Chebyshev coefficient $v_3$ represents intra-cycle shear thickening, an increase of viscous energy dissipation. This effect disappears with increasing strain and is replaced by intra-cycle strain-stiffening, an increase of the elastic response of the material. The negative minimum in $v_3$ at 200% strain suggest a strain shear thinning effect, the viscous dissipation slows down and the viscous 3rd harmonic contributions approach zero above 10 strain units.

Reporting the elastic and viscous modulus for various harmonics is confusing, as can be seen from figure 8. The higher order coefficients follow the trend of the 3rd order Fourier coefficients. The intensity of $G'_n$ and $G''_n$ decreases with increasing order, but no further insight is provided. Simple parameters combining the effects of all relevant Fourier coefficients, namely an elastic strain-stiffening/softening (S) and an viscous shear-thickening/thinning (T) ratios have been defined by Ewoldt *et al.* [5].

$$S \equiv \frac{G'_L - G'_M}{G'_L} = \frac{-4G'_3 + ..}{G'_1 - G'_3 + ..}$$

$$T \equiv \frac{\eta'_L - \eta'_M}{\eta'_L} = \frac{4G''_3 + ..}{G''_1 + G''_3 + ..} \qquad (8)$$

$G'_M$ is a minimum-strain and $G'_L$ a large-strain modulus representing local intercycle variations of the elastic behavior between small and large instantaneous strain. At the limit of small strain, $G'_M$ and $G'_L$ converge to the linear viscoelastic modulus $G'$. Along the same concept does $\eta'_M$ represent the minimum shear viscosity and $\eta'_L$ a large strain rate shear viscosity. In the linear region both S and T are equal to zero. S>0 corresponds to intra-cycle elastic stiffening and S<0 to intra-cycle softening. T>0 represents viscous intra-cycle shear thickening, T<0 intra-cycle shear thinning

Figure 9 shows for the Xanthan gum solution the variation of the strain stiffening/softening and the shear thickening/thinning ratio during the transition from low to large amplitude strain i.e. linear to nonlinear behavior.

At the onset of the nonlinear behavior, the Xanthan gum thickens (T>0), paralleled with a slight elastic softening (S<0). Beyond 40% strain, the material stiffens abruptly and S reaches a value of ~ 1.5; the

elastic contribution in the material increases sharply as the material is strained further. At the same time the shear thickening/ thinning ratio T decreases and falls below 0 at 200% strain. Between 100 and 500% strain, S remains constant, although exhibiting strong variations at high level. Beyond 500% strain, S decreases along with T; at this point the gel structure deteriorates very fast. A viscous thickening at the beginning of the nonlinear region can be expected from the peak in the loss modulus $G''_1$. Not apparent form the storage modulus $G'_1$ however is the strong elastic stiffening of the gel before the gel structure breaks apart. It should be noted, that the behavior of the elastic stiffening/softening ratio S follows the relative magnitude of the third order harmonic contribution in figure 3.

With the concept of intra-cycle elastic and viscous variations, the transition from linear to nonlinear behavior can be probed in more detail and structural changes investigated.

## CONCLUSION

The capability to perform highly accurate LAOS experiments on a commercial SMT (Separate Motor and Transducer) has been demonstrated. Expanding standard correlation techniques to provide not only the fundamental but also high order harmonic content in terms of magnitude and phase has proven to be an accurate and fast tool to analyze the nonlinear stress response. A typical viscoelastic gel, the 4wt% Xanthan gum solution has been tested and analyzed using the extended correlation technique. The raw strain and stress waveforms of the experiments were also analyzed using commonly used DFT techniques and a decomposition method proposed by Cho *et al.*[3]. Excellent agreement has been obtained between the 3 evaluation methods. Finally the results, represented here by the higher order Fourier coefficients $G'_n$ and $G''_n$ were interpreted in terms of elastic and viscous dissipation effects. Structural changes during the transition from linear to highly non linear behavior could be investigated in more detail.


## ACKNOWLEDGMENTS

The author would like to acknowledge Prof. M. Wilhelm and Ph.D. Candidate. R. Ewoldt for very helpful discussions.


## REFERENCES


1. A.D.Crowell, Am. J. Phys. **49,** 452 (1981)
2. Wilhelm, M. Reinheimer, P. Ortseifer, M. Spiess H.W. Rheol. Acta **38**, 349-356 (1999)
3. Cho, K.S. Ahn, K.H. Lee, S.J.. J.Rheol. **49**(3), 747-758 (2005)
4. Ewoldt, R.H. McKinley, G.H. Hosoi, A.E. Annual Transactions of the Nordic Rheology Society **15**, (2007)
5. Ewoldt, R.H. McKinley, G.H. Hosoi, A.E., *Fingerprinting Soft Materials: A Framework for Characterizing Nonlinear Viscoelasticity*.arXiv, 2007. **0710.5509v1**: [cond-mat.soft]
6. Krieger, I.M. , T.F.Niu, Rheol. Acta 12, 567-571(1973)
7. Giacomin A.J., J.M. Dealy, in Techniques in Rheological Measurements" edited by A.A. Collyer (Chapman and Hall, London, 1993), Chap. 4, pp. 99-121
8. Wilhelm, M. Reinheimer, P. Ortseifer, M. Spiess H.W. Rheol. Acta **38**, 349-356 (1999)]
9. Ewoldt, R.H., P. Winter, available from http://web.mit.edu/nnf/
10. Hyun, K.S., S.H. Kim, K.H. Ahn, S,J. Lee, Non-Newtonian Fluid Mech. **107**, 51-65 (2002)
11. Neidhöfer, T, M. Wilhelm, J.Rheol. **47** (6), 1351-1371 (2003)
12. Hyun, K., J.G.Nam, M.Wilhelm, K.H.Ahn, S.J.Lee, Korean-Australia Rheology J. **15**(2), 97-105 (2003)
13. Atalik, K, R.Keunings, J.NonNewtonian Fluid Mech. **122**, 107 (2004)
14. Graham, M.D. J.Rheol. **39**, 697 (1995)